A R C H I V E S O F M E T A L L U R G Y A N D M A T E R I A L S
Volume 60 2015 Issue 2
DOI: 10.1515/amm-2015-0104

H.-S KIM*, M. BABU*, S.-J. HONG*,♯

MICROSTRUCTURE AND THERMOELECTRIC PROPERTIES OF TAGS-90 COMPOUNDS FABRICATED BY MECHANICAL MILLING PROCESS

MIKROSTRUKTURA I WŁAŚCIWOŚCI TERMOELEKTRYCZNE ZWIĄZKÓW TAGS-90 WYTWORZONYCH PRZEZ MIELENIE

TAGS-90 compound powder was directly prepared from the elements by high-energy ball milling (HEBM) and subsequently consolidated by a spark plasma sintering (SPS). Effect of milling time on the microstructure and thermoelectric properties of the samples were investigated. The particle size of fabricated powders were decreased with increasing milling time, finally fine particles with ~1μm size was obtained at 90 min. The SPS samples exhibited higher relative densities (>99%) with fine grain size. X-ray diffraction analysis (XRD) and energy dispersion analysis (EDS) results revealed that all the samples were single phase of GeTe with exact composition. The electrical conductivity of samples were decreased with milling time, whereas Seebeck coefficient increased over the temperature range of RT~450°C. The highest power factor was 1.12×10^{-3}W/mK^2 obtained for the sample with 90 min milling at 450°C.

Keywords: TAGS-90, Thermoelectric properties, High-energy milling, SPS

1. Introduction

There are rapidly increasing global demands for environmental-friendly energy resources and alternative techniques as a solution for critical issues such as fossil fuels depletion, energy efficiency and global warming. To achieve this, solid-state thermoelectric (TE) conversion is amongst the best alternative energy technology because of its capability to directly convert heat to electricity and vice versa. The efficiency of a thermoelectric generator is determined mainly by material performance which is represented by the dimensionless thermoelectric figure of merit ZT = $(\alpha^2\sigma/\kappa)$ T, where α is the Seebeck coefficient, σ is the electrical conductivity, κ is the thermal conductivity, and T is the absolute temperature [1-3]. Most advances in recent studies as compared to conventional materials are on increasing the power factor $(\alpha^2\sigma)$ and decreasing the thermal conductivity (κ) [4, 5].

Many researchers have established TE materials such as Bi_2Te_3, Sb_2Te_3, SiGe, SnTe, TAGS and PbTe as the best performance materials for several decades, and these materials still continue to attract interest in TE research and industry [6]. Among these, the compound $(GeTe)_x(AgSbTe_2)_{100-x}$, commonly called TAGS-x has been given much attention for power generation from waste heat [7,8], because of its maximum ZT generation in 300~450°C temperature range, which is temperature range of automobile's exhaust gases and industrial waste heat [9].

Earlier research on TAGS materials focused on composition optimization, doping, and structural analysis. It was found that the TAGS system compositions present as a solid solution of GeTe and $AgSbTe_2$, and transport properties varied with their ratio. The compositions focused GeTe rich compositions; and subsequently studied on TAGS-80, TAGS-85 and TAGS-90 due to higher ZT value [10]. On the other hand, Doping and structural change yielded negligible effect on the transport properties [11, 12], but defects, nanoscale compositional modulations, nano domains, precipitate, twins, and grain boundaries showed remarkable effects [6, 12, 13]. As new approach, works based on defects can increase the Seebeck coefficient by enhancing scattering factor (g), and reducing thermal conductivity through enhanced phonon scattering, which serves as an effective way to improve the TE performance.

Material preparation methods are the most important role in TE materials performance. In general, TAGS materials are prepared through the casting and annealing, and the products of this method usually have good TE properties [11]. However, it needs long processing time and has poor mechanical properties as well. To rectify these shortcomings, powder metallurgy is really considered as a new favorable approach to prepare TE materials that can exhibit a good combination of TE performance and mechanical properties. Several efforts have been made to prepare efficient TE materials, however, combination of mechanical alloying (MA) and spark plasma sintering (SPS) is always a promising way for the preparation of TE materials [14, 15].

In recent years, MA and SPS processes are extensively used to fabricate various TE materials with fine microstructure. Furthermore, MA is a unique method and offers a sim-

* DIVISION OF ADVANCED MATERIALS ENGINEERING, KONGJU NATIONAL UNIVERSITY, CHEONAN, REPUBLIC OF KOREA
♯ Corresponding author: hongsj@kongju.ac.kr

ple synthesis process directly from elements of TE materials [16, 17]. But, there has not been any report of direct form of the TAGS preparation by MA and SPS even though this is a well-known material and these methods are less time consuming and inexpensive.

In present work, we prepared TAGS-90 alloys using MA and SPS, and investigated the effects of milling time(30, 60, 90 min) on the its microstructure and TE properties.

2. Experimental

High purity (>99.999%) elementary Ag, Sb, Ge, and Te granules of few mm size were weighed according to the required stoichiometric composition of p-type $(GeTe)_{90}(AgSbTe_2)_{10}$ named as TAGS-90 compound. The powder was fabricated directly from elements by high-energy ball milling (HEBM) process at different milling time of 30, 60, and 90 min. HEBM is a powerful and effective process method, which can fabricate alloy powders from raw elements in a short period of time [18]. Then as-milled powders were consolidated by spark plasma sintering (SPS) at 450°C, under pressure of 50MPa holding for 5 min in a vacuum. The densities of the resultant disks were measured by Archimedes method, the experiment was repeated 8 times and then obtained values were averaged.

The microstructure of both the powders and sintered samples were observed by scanning electron microscopy (SEM). The phase structure of samples were characterized by X-ray diffractometer (XRD) using high-energy monochromatic CuKα radiation (0.15418 nm) in the 2θ range of 20~80°. The particle size distribution analysis (PSA) was performed to confirm the size of milled powders.

The Seebeck coefficient and electrical conductivity were measured in the range of room temperature to 450°C using a commercial ZEPEL TEP-1000, which is controlled by computer aided programmer. The power factor was then calculated using PF = $\alpha^2\sigma$ and compared.

3. Results and discussion

Fig. 1 shows the XRD patterns of the mechanically alloyed TAGS-90 powders with different milling time. All the XRD peaks are indexed to the GeTe single phase, which is a mixture of the rhombohedral structure with a space group of R3m (JCPDF no. 47-1079) and the cubic structure with space group of Fm-3m (JCPDF 065-0305) [13, 19]. It is revealed that TAGS-90 compound powder was completely formed from the raw elements even after 30 min of short milling time, due to induction of high-energy by HEBM process. The peak broadening is increased with increasing milling time, which indicated that the decrease in powder size yielded fine microstructure refinement [16]. The inset in Fig. 1 shows an expanded view of diffraction angle from 41° to 44° for as milled powers with milling time. It can be clearly seen from the inset, (024) and (220) peaks did not separate completely, indicating that lattice parameters changed systematically by HEBM process [9]. Furthermore, the (024) peak shifted to high angle and (220) shifted towards low angle, tending to overlap with increasing milling time due to the gradual transformation of rhombohedral to cubic phase [20, 21]. This Behavior shows that the changes in crystal structure of TAGS compounds were affected by the fabrication process and also microstructure refinement.

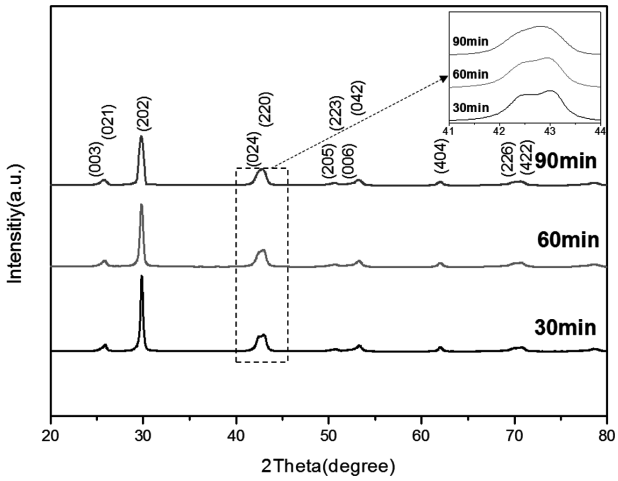

Fig. 1. Powder XRD patterns of TAGS-90 with milling time indicate the single GeTe with rhombohedral phase. The inserted patterns shows the shift of (024) and (220) peak positions with increasing milling time

Fig. 2. shows the SEM images and particle size distribution of the milled TAGS-90 powders after different milling times. Fig. 2(a) reveals that, how the initial large sized raw materials rapidly decreased in size after milling for 30 min. As milled powder exhibited not only agglomerated particles, that consisted fine particles of size around 2 μm to 3μm, but also observed few partially large particles around 10-15 μm. With increasing the milling time from 30 to 60min (Fig. 2(b)), the particle size decreased and refined more. Further milling up to 90min yielded the particles with fine size distribution about 500 nm to 1 μm, as shown in Fig. 2(c). It can be keenly observed that the smaller particles were and agglomerated due to cold welding of fine particles during the ball milling process. For further confirmation, Particle size distribution analysis (PSA) was performed. It is clearly shown in Fig. 2(d) that the particle size (agglomerated and fine particles) decreases with increasing milling time which is also confirmed by SEM images.

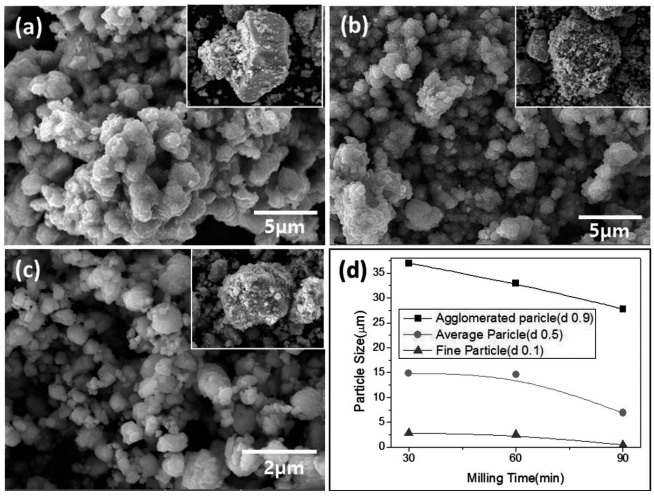

Fig. 2. SEM image of as milled TAGS-90 powders with milling time; (a) 30min, (b) 60min, (c) 90min, and (d) particle size distribution

Fig. 3. illustrates the fractured surfaces of sintered bulk samples obtained from milling of powder for 30, 60, and 90min. The TAGS-90 bulk specimens prepared by the SPS, had high relative densities (>99%) of its theoretical density and observed the grain growth than milled powders, but were reasonably fine. As shown in Fig.3(a), the several large grains about 15 μm were observed in 30min sample. With increasing milling time to 60min (Fig. 3(b)), the number of the large grains were decreased and homogenized, subsequently, fine grains of ~2 μm with no large grains were observed in 90min milling sample (Fig. 3(c)).

Fig. 3(d) shows the energy dispersive spectroscopy (EDS) analysis of milled powder and sintered bulk samples prepared from 90min milling. According to the table in Fig 3(d)), the initial composition is approximately coinciding with final nominal composition of TAGS-90 compound. In addition, all samples have less or almost no impurity and oxygen content even after milling for 90 min. Thus the conclusive remarks from these results are that highly dense, fine grains and pure TAGS-90 bulk samples were prepared using HEBM and SPS methods.

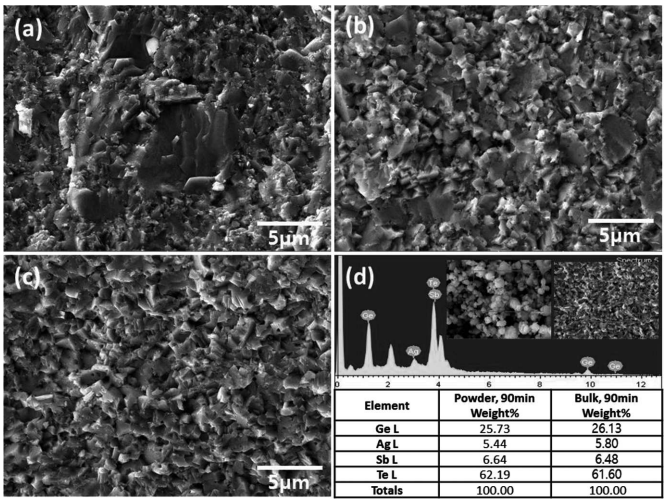

Element	Powder, 90min Weight%	Bulk, 90min Weight%
Ge L	25.73	26.13
Ag L	5.44	5.80
Sb L	6.64	6.48
Te L	62.19	61.60
Totals	100.00	100.00

Fig. 3. SEM images of fractured surface of the bulk TAGS-90 samples obtained from milled powders for (a) 30min, (b) 60min, (c) 90min., and (d) composition of milled and sintered bulk samples at 90min of milling time

The temperature dependences of electrical conductivity (σ), Seebeck coefficient (α), and power factor ($\alpha^2\sigma$) from RT to 450°C are shown in Fig. 4(a)-(c), respectively. The electrical conductivity of all samples decreased with increasing temperature up to 300°C, then slightly increased at 350°C and decreased again as shown in Fig. 4(a). This discontinuity in electrical conductivity is owing to the phase transformation of rhomobohedral to cubic polymorphic in general TAGS system [22]. Interestingly, the phase transition regions decreases and moves to lower temperature as the milling time increases.

The electrical conductivity of all samples decreased with increasing milling time. In general, the electrical conductivity is a combination of the carrier concentration and mobility expressed by $\sigma = \mu e n_c$. Where, μ is mobility, e is charge of the electron and n_c is number of charge carriers in the system. It is known that the mobility is greatly influenced by the grain boundary scattering [23]. TAGS materials behave as a native strong p-type because of the carrier from defect structure [11, 24]. It is known that the carrier concentration increases with increasing defects in the matrix, and these induced charge carriers causes the carrier-carrier scattering, which reduces carrier transportation and mobility. Despite having higher carrier concentration from increased number of defects, the samples showed lower electrical conductivity as milling time was increased; it can be attributed to the reduction of the mobility by smaller grain size and carrier scattering mechanism.

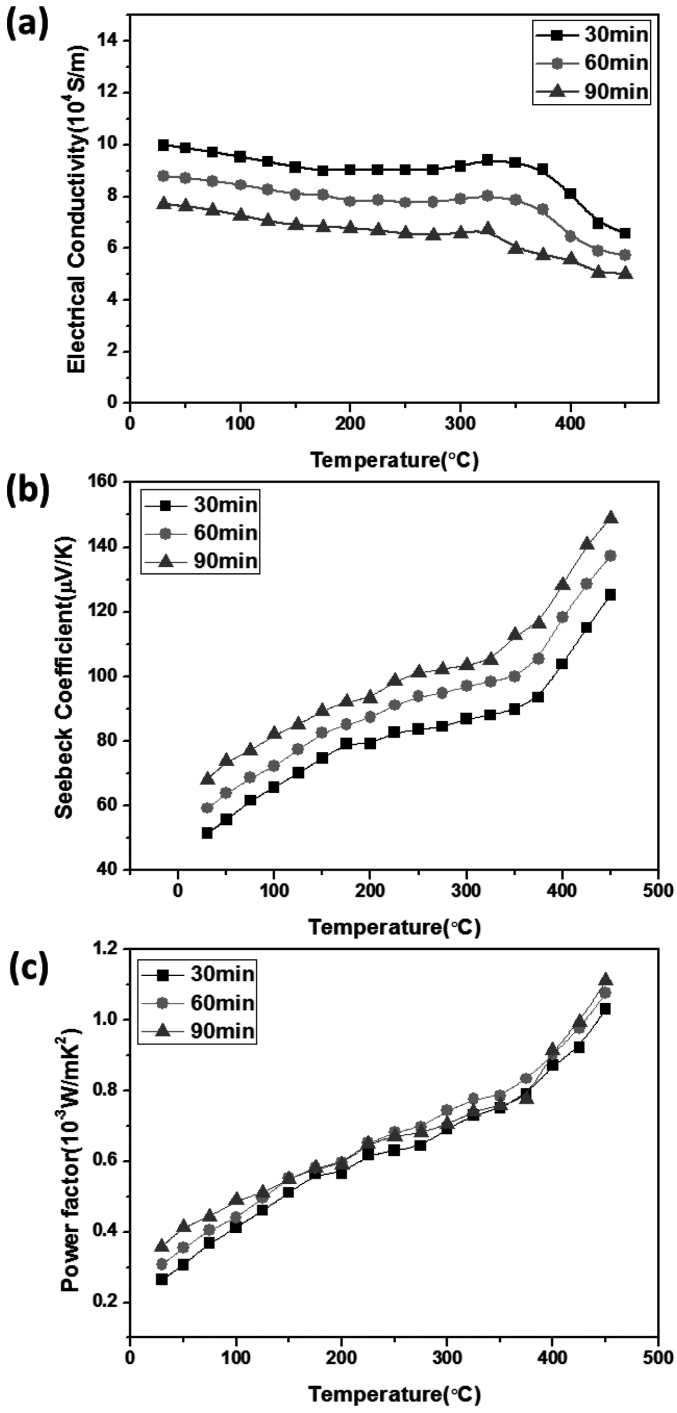

Fig. 4. Temperature-dependence of (a) electrical conductivity, (b) Seebeck coefficient, and (c) power factor for TAGS-90 samples prepared by different milling time and sintered at 450°C

The Seebeck coefficients of all sintered samples were positive throughout the measured temperature range i.e. RT to 450°C as shown in Fig. 4 (b), which means that TAGS-90

compounds behaved as a p-type semiconductor and the holes were the majority charge carriers. The Seebeck coefficient of all samples were increased in temperature range from RT to 450°C, however slight deviations in slopes can be observed at 300-350°C temperature region which is due to the phase transition as explained in previous paragraph. In addition, Seebeck coefficient values of samples increased with increasing milling time. The Seebeck coefficient can be expressed by $\alpha = Y - \ln n_c$, where Y is the scattering factor. Several scattering mechanisms could affect the Seebeck coefficient, for example, grain boundary scattering, impurity scattering, phonon scattering, and carrier scattering [23]. From the results showing changes in microstructure, as shown in Fig. 3, we can expect that the Seebeck coefficient was affected by grain size. Therefore, it is considered that the grain boundary scattering is likely to be primary scattering mechanism in these samples. The highest Seebeck coefficient value amongst the samples was 149μV/K at 450°C obtained from 90 min milling powders.

The power factor was calculated as PF = $\alpha^2\sigma$ from the results of the Seebeck coefficient and the electrical conductivity of samples. Fig. 4 (c) shows the temperature dependence of the power factor of samples with different milling time. There was no large difference in power factor for different milling time. The highest power factor obtained was 1.12×10^{-3}W/mK^2 at 450°C for the sample prepared from 90 min of milling. Although this sample had the highest power factor, it is slightly lower than the previous reported values but still reasonable [13].

4. Conclusions

TAGS-90 TE materials with fine grains were successfully prepared by HEBM and SPS processes, and then the effect of milling time on the microstructure and transport properties was studied. The samples had exact composition, high relative densities (>99%), and fine grain sizes. Increasing milling time reduced the grain size, increased the Seebeck coefficient values and decreased the electrical conductivity. The highest power factor was 1.12×10^{-3}W/mK^2 obtained at 450°C for sample prepared by using 90 min milling powder. From the results, we conclude, the combination of HEBM and SPS is a new simple and reliable fabrication method for producing TAGS-90 TE materials directly from elements in a short time at very inexpensive cost.

Acknowledgements

This research was supported by Basic Science Research Program through the National Research Foundation of Korea (NRF) funded by the Ministry of Education, Science and Technology (2012R1A1A2008113), and also part of this work was supported by the Korea Institute of Energy Technology Evaluation and Planning (KETEP) grant funded by the Korea government Ministry of Knowledge Economy (No. 2011501010020).

REFERENCES

[1] T.M. Tritt, Science **283**, 804 (1999).
[2] B.C. Sales, D. Mandrus, E. Siivola, T. Colpitts, B. Q'Quinn, nature, **413**, 597 (2001).
[3] F. Ioffe, Semiconductor Thermoelements and Thermoelectric Refrigeration, P. 39, Infosearch, London (1957).
[4] M.S. Dresselhaus, G. Chen, M.Y. Tang, R. Yang, H. Lee, D. Wang, Z. Ren, J.P. Fleurial, P. Gogna, Adv. Mater. **19**, 1043 (2007).
[5] B.C. Slaes, D. Mandrus, R.K. Williams, Science **272**, 1325 (1996).
[6] B.A. Cook, M.J. Kramer, X. Wei, J.L. Harringa, J. Appl. Phys. **101**, 053715 (2007).
[7] D. Rosi, J.P. Dismuke, E.F. Hockings, Electr. Eng. **79**, 450 (1960).
[8] G.C. Christakudis, S.K. Plachkova, L.E. Shelimova, E.S. Avilov, Phys. Staus, Solidi A 128, 465 (1991).
[9] Y.K. Dong, A.-S. Malik, F.J. Disalvo, J. Electron. Mater. **40**, 17 (2011).
[10] E.A. Skrabek, D.S. Trimmer, U.S. Patent No. 3,945,855 (23 March 1976).
[11] E.A. Skrabek, D.S. Trimmer, CRC Handbook of Thermoelectrics (ed., D. M. Rowe), p. 267, CRC, Boca Raton, FL (1995).
[12] B.A. Cook, X. Wei, J.L. Harringa, M.J. Kramer, J. Mater. Sci. **42**, 7643 (2007).
[13] S.H. Yang, T.J. Zhu, T. Sun, J. He, S.N. Zhang, X.B. Zhao, Nanotechnology **19**, 245707 (2008).
[14] J.H. Son, M.W. Oh, B.S. Kim, S.D. Park, B.K. Min, M.H. Kim, H.W. Lee, J. Alloys Compd. **566**, 168 (2013).
[15] S.S. Lin, C.N. Liao, J. Appl. Phys. **110**, 093707 (2011).
[16] M. Zakery, M. Allahkarami, Gh. Kavei, A. Khanmohammadian, M.R. Rahimipour, J. Mater. Process. Tech. **209**, 96 (2009).
[17] C.H. Kuo, H.-S. Chien, C.-S. Hwang, Y.-W. Chou, M.-S. Jeng, M. Yoshimura, Materials Transactions **52**, 795 (2011).
[18] H.S. Kim, C.M. Kim, C.H. Lee, S.K. Lee, H.S. Hong, J.M. Koo, S.J. Hong, J. Kor. Powd. Met. Inst. **20**, 107 (2013).
[19] S.N. Zhang, J. He, X.H. Ji, Z. Su, S.H. Yang, T.J. Zhu, X.B. Zhao, T.M. Tritt, J. Electron. Mater. **38**, 1142 (2009).
[20] E.M. Levin, B.A. Cook, J.L. Harringa, S.L. Bud'ko, R. Venkatasubramanian, K. Schmidt-Rohr, Adv. Funct. Mater. **21**, 441 (2011).
[21] H.S. Kim, J.K. Lee, J.M. Koo, B.S. Chun, S.J. Hong, J. Kor. Powd. Met. Inst. **18**, 449 (2011).
[22] J.R. Salvador, J. Yang, X. Shi, H. Wang, A.A. Wereszczak, J. Solid State Chem. **182**, 2088 (2009).
[23] J. Bardeen, W. Shockley, Phys. Rev. **80**, 72 (1950).
[24] N.V. Kolomoets, E. Ya. Lev, L.M. Sysoeva, Soviet Phys. Solid State **5**, 2101 (1964).

Received: 20 November 2014.